

Supporting Information

Supporting Information

**Individually Addressable Arrays of Replica Microbial Cultures Enabled by Splitting SlipChips**

*Liang Ma, Sujit S. Datta, Mikhail A. Karymov, Qichao Pan, Stefano Begolo, and Rustem F. Ismagilov\**

\*Corresponding author: rustem.admin@caltech.edu

**Supplementary Methods**

**Materials**

All reagents were purchased from commercial sources and used without further purification unless otherwise stated.

FC-40 (a mixture of perfluoro-tri-n-butylamine and perfluoro-di-nbutylmethylamine) was obtained from 3M. Thirty-gauge Teflon tubing was obtained from Weico Wire & Cable. Gastight syringes were obtained from Hamilton Company. Poly(dimethylsiloxane) (PDMS, Sylgard 184 Silicone Elastomer kit) was obtained from Dow Corning. (tridecafluoro-1,1,2,2,-tetrahydrooctyl)-1 trichlorosilane was obtained from United Chemical Technologies. Sucrose was obtained from Fisher Scientific.

Photomasks were designed in AutoCAD and ordered from CAD/Art Services, Inc. (Bandon, OR). Soda-lime glass plates with chromium /photoresist and chromium /gold/photoresist coating were purchased from Telic Company (Valencia, CA). Through holes were drilled in the top plate with a 0.035" drill bit from Colmar Industrial Supplies (Wheeling, IL).

Stainless steel sheets and pins were purchased from McMaster-Carr (Elmhurst, IL). Binder clips (5/32' inch capacity, 1/2' inch size) were purchased from OfficeMax (Itasca, IL). Cooked Meat Medium, Wilkins-Chalgren anaerobe broth, Difco Luria-Bertani broth medium (LB), Noble agar,

## Supporting Information

and tetradecane were purchased from Fisher Scientific (Hanover Park, IL). Ultra-low gelling temperature Type IX-A agarose, gold etchant, and dichlorodimethylsilane were purchased from Sigma-Aldrich (St. Louis, MO).

*Bacteroides thetaiotaomicron* (*B. theta*) was purchased from ATCC. Echo therm chilling plate was purchased from Torrey Pines Scientific (Carlsbad, CA).

Primers for PCR were ordered from Integrated DNA Technologies (Coralville, IA). SsoFast EvaGreen Supermix (2X) was purchased from Bio-Rad Laboratories (Hercules, CA). Bovine serum albumin solution (BSA) was purchased from Roche Diagnostics (Indianapolis, IN). PCR Mastercycler and in situ adapter were purchased from Eppendorf (Hamburg, Germany).

### Homemade Reagents:

A protocol for making GBSS buffer and AM2 medium can be found from the Schmidt Lab website.<sup>1</sup> For H<sub>2</sub>Oc or PBSc, 0.2% cysteine was added and the solution was sterilely filtered through 0.22 μm membrane. Tetradecane was sterilely filtered through 0.22 μm membrane (Fisher Scientific). 0.1 M Fe(SCN)<sub>3</sub> solution was sterilely filtered through 0.22 μm membrane (Fisher Scientific) and used as a red dye solution. 60% (w/w) sucrose solution with red dye was prepared by dissolving 600 mg crystals of sucrose into 400 mg of 0.1 M Fe(SCN)<sub>3</sub> solution. Filtered tetradecane was degassed under house vacuum overnight and used to assemble SlipChips for depositing PCR reagents. All plastic consumables and reagents were equilibrated in an anaerobic chamber for more than 24 hours before usage.

## Methods

### Design and fabrication of SlipChip

On the replica-SlipChip for cultivation, each plate contained both wells and channels while on SlipChips for depositing PCR reagents, each plate contained either wells or channels but not

## Supporting Information

both. SlipChips were fabricated as previously reported<sup>2</sup> with the following modification: for devices with cultivation wells and PCR reagent wells, soda-lime glass plates with chromium/gold/photoresist coating were used.

### Dimensions for the device

The depths of the features measured by a contact profiler (Dektak 150, Veeco, CA) were 90  $\mu\text{m}$  for replica chip, 120  $\mu\text{m}$  for PCR reagent wells, and 60  $\mu\text{m}$  for loading channels of the PCR SlipChip. The lateral dimensions of cultivation and PCR reagent wells can be measured by photographs from a stereoscope, as shown in Fig. 2 and Fig. S7, respectively.

### Using continuous channels to promote gas exchange

The concentration of gas molecules in the liquid cultivation medium in equilibrium is described by Henry's law:  $c = p/k_H$ , where  $c$  [ $\text{mol L}^{-1}$ ] is the concentration of the solute in the solution phase,  $p$  [Pa] is the partial pressure of the solute molecule in the gas phase, and  $k_H$  [ $\text{Pa L mol}^{-1}$ ] is the Henry's law constant. The previously reported SlipChips are capable of handling only two phases: the aqueous phase and the oil phase.<sup>3</sup> As the SlipChip is fabricated in glass, which is not gas permeable, transport of gas can only happen by diffusion through the oil in the gap. The characteristic diffusion time of gas through the lubricating oil phase in the gap  $t_d$  [s] is given by  $t_d = L^2/2D$ , where  $D$  [ $\text{m}^2\text{s}^{-1}$ ] is the diffusion coefficient of the gas molecule, and  $L$  [m] is the characteristic length scale. For example, the diffusion coefficient for oxygen in hydrocarbon<sup>4</sup> is reported to be  $\sim 10^{-9} \text{ m}^2\text{s}^{-1}$ . For a device on the centimeter scale, the characteristic diffusion time for oxygen can be as long as several hours or even a day.

We incorporated gas supply channels in the design to promote gas exchange between the microwell and ambient atmosphere (Fig. S2 and S3). The distance between the channels and wells is on the order of hundreds of microns, which shortens the characteristic diffusion time to minutes.

## Supporting Information

In this design, gas is introduced into the loading channel by removing the fluid with a vacuum. Since the SlipChip is not bonded, the gap between the two halves can serve as an oil reservoir, and we observed that oil flowed back to the channel when the vacuum was released. In order to maintain the gas supply and prevent oil from flowing back into the channel, we repeated purging and found that purging three to five times before loading the sample (Fig. 2(a)) prevented oil from entering the channel during cultivation.

### **Fabrication of a glass slide with index for the replica-SlipChip**

The index for each well on the replica-SlipChip was created with AutoCAD and this design was used to prepare a photomask. The feature was then transferred by photolithography to a soda-lime glass plate with chromium/photoresist coating. The photoresist and chromium in exposed region were then etched away, and unexposed photoresist was then removed by ethanol. The chromium under the unexposed region serves as index for each well (Fig. S8, numbers in dark are chromium layer).

### **Fabrication of the holder**

The holder (Fig. S4) for the SlipChip was fabricated by standard machining. Three pins for aligning SlipChips were inserted into the holder. Two glass spacers between the holder and the top plate were made by cutting 1 mm thick microscope slides into small pieces and glued to the holder on the edges with 5-min epoxy. The edge of the bottom plate was also removed to fit into the bottom part the holder with the glass spacer. The center part of the holder was cut away to facilitate imaging.

### **Through holes with defined size and position on SlipChip**

Through holes used to align the SlipChip (Fig. S3) to the holder were fabricated on both replica-SlipChips and PCR chips. Markers to define positions for through holes were incorporated into the design of photomasks and then transferred to the device by photolithography and wet-

## Supporting Information

etching. To fabricate through holes, the device was first aligned to the laser stage using the etched marker, then ablated by laser machining (Resonetics RapidX250 system) with constant energy mode of 100 mJ with repetition rate of 80 Hz using 75-mm lens.

### **Cleaning and surface modification**

Prior to use, the SlipChips were cleaned with piranha solution and silanized with dimethyldichlorosilane using a previously reported protocol.<sup>2</sup>

### **Design and fabrication of PDMS microfluidic devices**

Multi-height SU8 masters were designed in Autocad. The features for the wells are taller than the ones for channels. The width of the rectangular channel is 550  $\mu\text{m}$ . The diameter of the circular well is 400  $\mu\text{m}$ , with a  $\sim 20\text{-}\mu\text{m}$  overlap with the main channel. The overlap ensured that the features for the wells made contact with the channels during fabrication. Microchannels with rectangular cross-sections were fabricated with rapid prototyping<sup>5</sup>. The wafer was aligned to the second photomask for the wells using a Suss MJB3 mask aligner. The heights of the features were measured by a contact profiler (Dektak 150, Veeco, CA). We fabricated molds at three different depths for channels: 34  $\mu\text{m}$ , 45  $\mu\text{m}$  and 77  $\mu\text{m}$  while keeping the height for the wells constant at 180  $\mu\text{m}$ . The PDMS microfluidic devices consisted of PDMS microchannels functionalized with (tridecafluoro1,1,2,2-tetrahydrooctyl)-1-trichlorosilane to render them hydrophobic and fluorophilic.<sup>6</sup>

### **Understanding the splitting process with a model system on a PDMS device**

Carrier fluid of FC40 was loaded into 1001 series Gastight syringes (Hamilton, Reno, NV) with removable 27-gauge needles and 30-gauge Teflon tubing (Weico Wire & Cable, Edgewood, NY). A plug of aqueous solution with additional carrier fluid was aspirated into the tubing under carrier fluid to avoid trapping of air bubbles. The PDMS channel and well was flushed with

## Supporting Information

carrier fluid to remove the air. The aqueous phase was then introduced into the well. Excess aqueous solution was removed by gently flowing carrier fluid.

The volumetric flow rate and duration of the flow was controlled using Harvard syringe pump under the volume mode. Images were taken using Leica MZ 16 stereoscope, collected with SPOT Advanced software and processed with ImageJ.

### Surface tension measurement

The surface tension of aqueous solution in fluorocarbon was measured as previously reported<sup>7</sup> with some modifications. Surface tension measurements of aqueous droplets in oil were made using a Rame-Hart Instrument Co. goniometer (model 500-00 Advanced). The goniometer was calibrated with 4 mm spherical standard. The surface tension was measured under a bath of FC40 in a transparent cuvette. Aqueous solution of 0.1 M Fe(SCN)<sub>3</sub> was loaded into a 1 mL syringe (BD) and passed through a blunt end metal 21 gauge needle (Zephyrtronics, cat #: ZT-5-021-5-L). A through hole was punched at the bottom of the cuvette. The needle was introduced into the cuvette and the cuvette was sealed with 5-min epoxy. The droplet of aqueous solution in FC40 was imaged and analyzed using DROPimage Advanced software (Rame-Hart Instrument Co).

### Contact angle measurement

We measured the contact angle formed between the aqueous phase of 0.1 M Fe(SCN)<sub>3</sub> solution, the lubricating FC-40 oil, and the silanized PDMS channel used in the model experiment with a direct approach. Droplets were formed by de-wetting after the passage of a slug of the aqueous phase. Images of nine different aqueous droplets were acquired using a Leica MZ 16 stereoscope equipped with SPOT Advanced software. We detected the edges of the droplets using ImageJ, and directly measured the local three-phase contact angle of the static droplets. The standard deviation of the measured contact angle is 8 degrees, which potentially reflects both variations in

## Supporting Information

the contact angle (e.g., due to surface heterogeneities) and the measurement error using this protocol.

**Calculation of viscous pressure drop in model PDMS device**

We used COMSOL multiphysics to perform a finite element simulation of laminar flow through a model PDMS device (using the exact 3D geometry as in the experiments described in the main text), with the fluid flowing through the gap and around a droplet in the well. An example is shown in Fig. S9. Our goal was to quantify how droplet trapping in the well modifies the flow behavior through the rectangular channel. For simplicity, we treated the droplet as a solid cylinder that completely fills the well, and did not incorporate the viscosity of the droplet, its wetting on the glass, or any flow-induced changes in the droplet geometry. For each geometry used in the experiments, we simulated the flow at a low flow speed 0.001 m/s, using a mesh size of approximately 8 $\mu\text{m}$ . At the low Reynolds numbers characterizing our experiments, the volumetric flow rate  $Q$  through the channel, around the trapped droplet, is proportional to the pressure drop across the droplet,  $P_{\text{visc}} = \mu(Q/A)L/k$ , where  $\mu$  is the viscosity of the flowing continuous phase,  $L$  is the length of the well (as depicted in Fig. 3(b) of the main text),  $A$  is the cross-sectional area of the channel, and we refer to  $k$  as the permeability – this quantifies how the geometry of the droplet that occludes the channel modifies the flow through it. We used our simulations to calculate  $k = \mu(Q/A)L/P_{\text{visc}}$  for the geometry specific to each experiment, using the given values of  $\mu$ ,  $Q$ ,  $A$ ,  $L$ , and the value of  $P_{\text{visc}}$  calculated from the simulation. We thereby calculate the viscous pressure drop  $P_{\text{visc}}$  across the trapped droplet for each value of  $Q$  explored in the experiments—this is represented by the horizontal axis in Fig. 3(b)(ii) of the main text. As described in the main text, we expected that the lateral motion of the droplets out of the wells was due to the flow of the lubricating oil that arises as the two halves of the device are separated. In particular, for a sufficiently long experimental time scale, a droplet is pushed out of its well if the viscous pressure drop across the droplet,  $P_{\text{visc}}$ , is larger than the threshold capillary pressure holding it in place,  $P_{\text{cap}}$ . As described in the main text, we experimentally find that the droplet is

## Supporting Information

pushed out when  $P_{visc} \approx 4P_{cap}$ , for an experimental time scale of 10s, similar to the time required to split the SlipChip device. We expect that this threshold would decrease to  $P_{visc} \approx P_{cap}$  for even longer experimental time scales, not explored here.

### Viscosity measurement

The viscosity was Newtonian over the range of shear rates 1-500 Hz. We used a 50-mm parallel plate geometry on a TA ARES strain-controlled rheometer. The viscosity of the sucrose was 80.3 +/- 0.5 mPa-s. The gap size was 350  $\mu$ m for the sucrose.

### Anaerobic chamber

Coy lab anaerobic chamber equipped with dehumidifier was used in all anaerobic cultivation experiments. The hydrogen level was maintained at 3–4% and relative humidity at 30%.

### Imaging growth of *B. theta*

We monitored the growth of *B. theta* using the following protocol to take devices out of the anaerobic chamber while protecting them from oxygen. Devices were put under  $H_2O_c$  in a Petri dish. The Petri dish was then sealed with Vaseline and Parafilm. Bright field images were taken by Leica DMI6000 microscope (Leica Microsystems) with a 20  $\times$  0.4 Leica objective and a Hamamatsu ORCA-ER camera with 1 $\times$  coupler. The device was then brought back to the anaerobic chamber in a GasPak system. Dry ice and water were placed at the bottom of the gaspak to generate  $CO_2$ . The gaspak was sealed during purging in the airlock.

### Imaging growth of the clinical sample

A microbial suspension obtained from a mucosal biopsy from the colon of a healthy human volunteer was cultivated using a homemade AM2 medium supplemented with 0.5% ultra-low gelling temperature agarose on replica-SlipChip. The SlipChip was incubated at 37  $^{\circ}C$  in an

## Supporting Information

anaerobic chamber for 8 days at Dr. Schmidt's lab. Bright field images were taken by Leica DMI6000 microscope (Leica Microsystems) with a  $20 \times 0.4$  NA Leica objective and a Hamamatsu ORCA-ER camera with  $1 \times$  coupler.

### **Handling frozen stock solutions of bacterial samples in anaerobic chamber**

Aliquots of 50  $\mu\text{L}$  were stored in  $-80$  °C freezer. The sample was transferred from the freezer to an anaerobic chamber on dry ice with GasPak systems.

### **Identifying *B. vulgatus* in WCA agar by Plate Wash PCR (PWPCR)**

Plate wash PCR was used to detect *B. vulgatus* on Wilkins-Chalgren anaerobe (WCA) agar plates following a previously described protocol<sup>8</sup> with minor modifications. Cell scrapers were used to collect cultivar of a frozen microbial suspension obtained from a mucosal biopsy from the colon of a healthy human volunteer on the plate. DNA was purified from pooled cell using QiaAmp DNA Mini kit. 50 ng of DNA and *B. vulgatus*-specific primers<sup>9</sup> were used for PCR.

### **Depositing PCR reagents on PCR chip**

The reaction master mixture was prepared by mixing 100  $\mu\text{L}$  of 2X SsoFast EvaGreen Supermix, 1  $\mu\text{L}$  of forward and reverse primer ( $100 \mu\text{mol L}^{-1}$ ), 10  $\mu\text{L}$  of  $10 \mu\text{g mL}^{-1}$  BSA solution, and 68  $\mu\text{L}$  of 2.5% (w/v) ultra-low gelling temperature agarose in water. This mixture was then loaded onto the SlipChip for depositing PCR reagents by replacing tetradecane in loading channels and this SlipChip was split to obtain 1,000 droplets deposited on one half of the SlipChip.

### **Combining replica chip with PCR chip**

The chip preloaded with PCR reagents was taken off the holder and combined with the cultivation chip by aligning through-holes with the pins. A binder clip was used to clamp the two plates together, allowing the combined SlipChip to be removed from the oil.

## Supporting Information

**Fluorescence imaging of PCR results**

Fluorescence images were acquired with a Leica DMI6000 microscope (Leica Microsystems) with a 10 x/0.4NA Leica objective and a Hamamatsu ORCA-ER camera with 1× coupler. An L5 filter with an exposure time of 500 ms was used to collect images. For quantitative analysis, fluorescent intensity of a fluorescence reference slide for L5 filter was recorded and used for background correction. Images were acquired and analyzed by using Metamorph imaging system version 6.3r1 (Universal Imaging) and ImageJ by the National Institutes of Health (<http://rsb.info.nih.gov/ij/download.html>).

**Sequencing PCR products and data analysis**

PCR products were sequenced by Laragen, Inc. (Culver City, CA) using BaVUL-F or 8F as a sequencing primer. The results were manually trimmed and edited in FinchTV (Geospiza) and analyzed by BLAST (National Center for Biotechnology Information). Sequencing data are provided below. From the three isolates we obtained and sequenced, we used LM\_BV1 for Fig. 6(b).

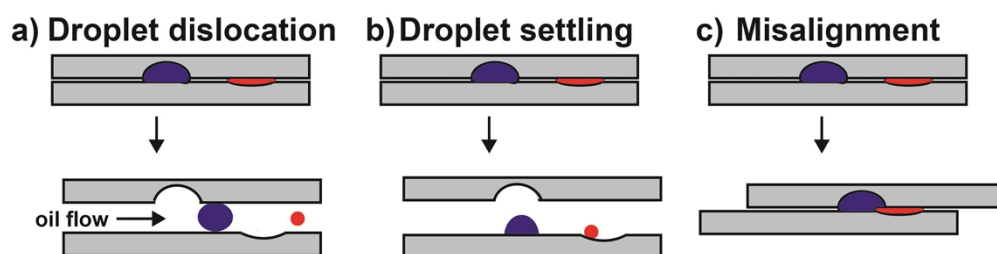
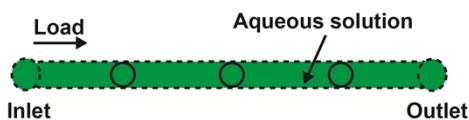


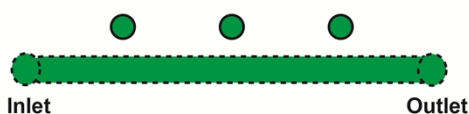
**Fig. S1.** Schematics showing various processes happening to droplets during splitting. (a) The droplets may be pushed out of the wells due to the presence of spontaneous oil flow. Oil flow is induced by separating the two plates vertically. (b) The droplets may settle to the bottom plate due to gravity. (c) The droplets from top and bottom plates may be brought together due to misalignment of the two plates.

## Supporting Information

## a) Load reagent



## b) Slip the dash layer downward



## c) Remove aqueous solution in the channel by a vacuum and load with lubricating oil

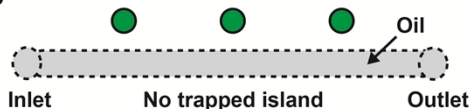


**Fig. S2** Schematic drawing of using continuous channel to remove trapped aqueous solutions. A) A continuous channel is used to load the aqueous solution into the circular wells. B) Slipping the dashed layer downward confines the aqueous solution in the wells. C) Purging the continuous channel with a vacuum removes residual aqueous solution in the channel. The channel is then filled with lubricating oil.

## Supporting Information

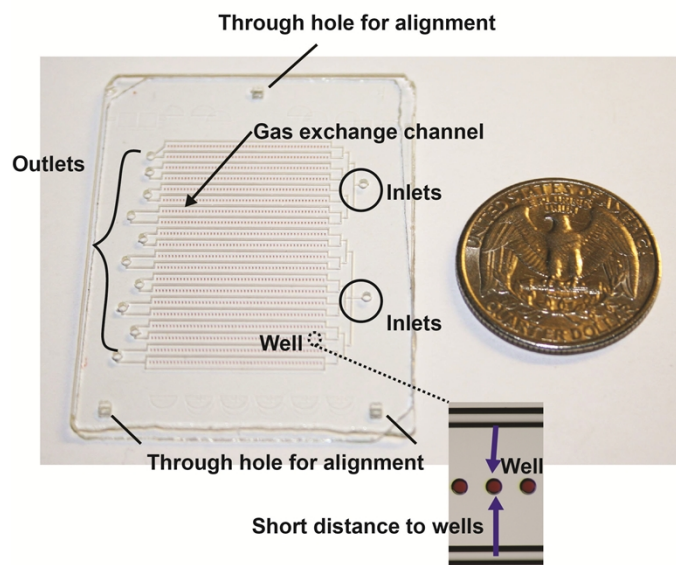


**Fig. S3** Representative photographs of current design of replica-SlipChip shown next to a U.S. quarter. In current design of replica-SlipChip, gas diffuses through the gap between the continuous channel and the wells, as shown in the inset. The continuous channel provides rapid and uniform gas exchange between the well and the channel. A representative image was used as an inset and may not be taken from the location as indicated by the dashed line.

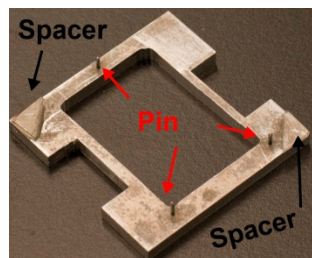


**Fig. S4** Photograph of holder with three pins for alignment and two glass spacers for splitting SlipChip.

## Supporting Information

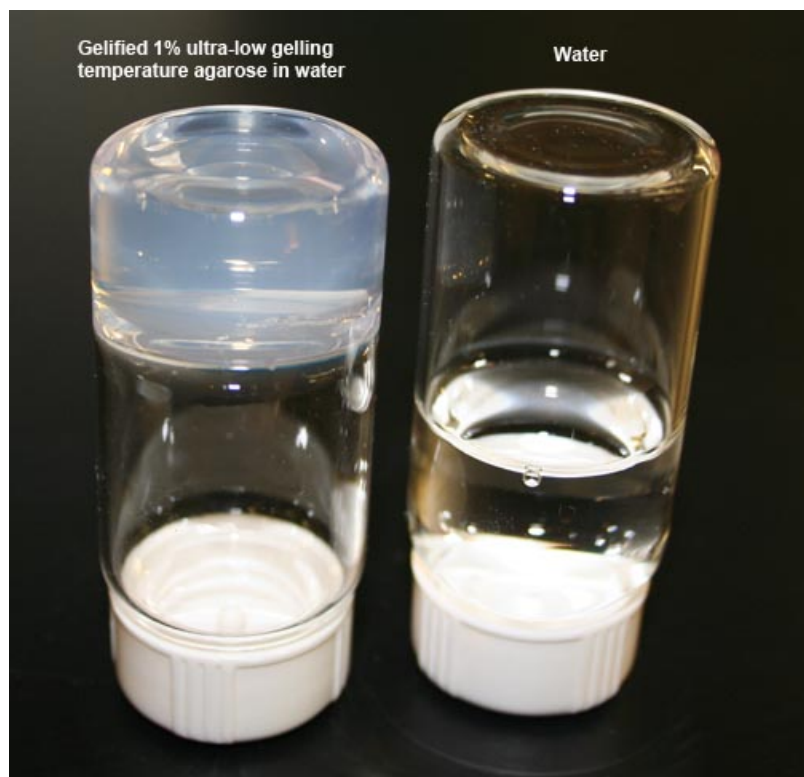


**Fig. S5** Photograph showing gelified 1% ultra-low gelling temperature agarose in water (left) sticking to the bottom of an inverted scintillation vial, while water (right) falls to the top of an inverted scintillation vial due to gravity.

## Supporting Information

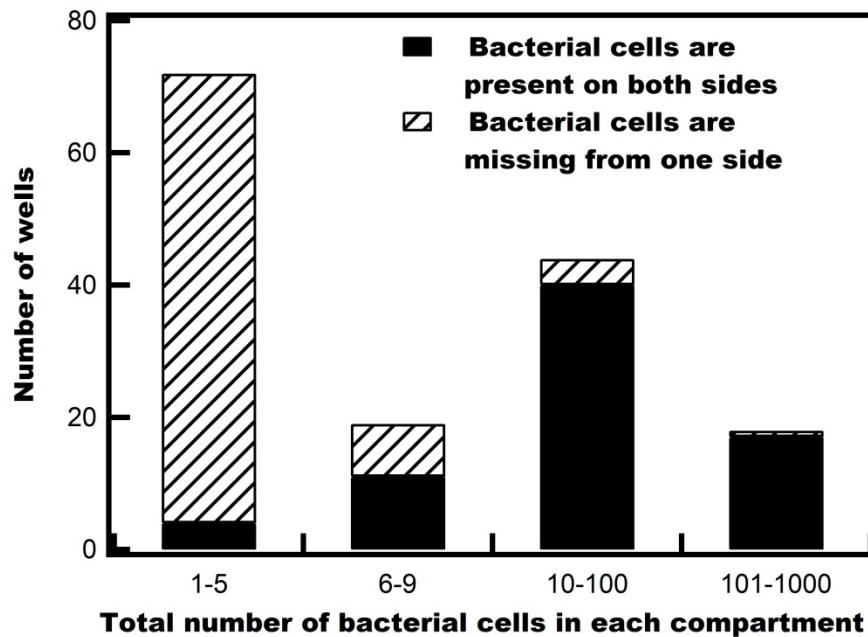


**Fig. S6** A plot showing distribution of bacterial cells on two sides of a SlipChip after separating each compartment by slipping. A microbial suspension obtained from a mucosal biopsy from the colon of a healthy human volunteer was cultivated using a homemade AM2 medium supplemented with 0.5% ultra-low gelling temperature agarose on replica-SlipChip. The dark bar indicates that bacterial cells were observed on both sides of the device. The hatched bar indicates that bacterial cells were observed only on one side of the device and were missing from the other side. Slipping successfully generates daughter colonies on both sides if the original compartment consists of a total of more than 10 cells.

## Supporting Information

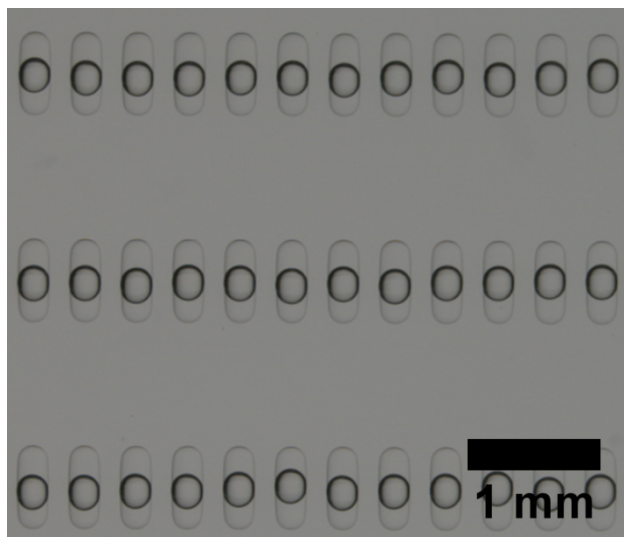


**Fig. S7** A photograph showing deposited droplets of 1% agarose aqueous solution on the half of the SlipChip used for PCR. The droplet shape changed after splitting.

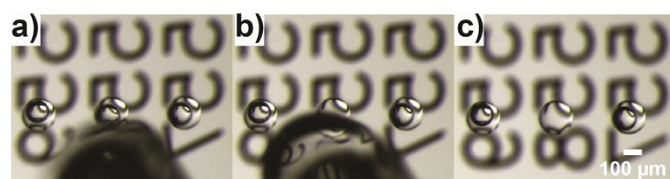


**Fig. S8** (a) A pipette loaded with buffer was placed near the micro-colony of interest (in this case, located in well number 558). (b) A ~2 nL droplet of 1% agarose aqueous solution merged spontaneously with 1 μL GBSS buffer. (c) The combined solution was then aspirated back into the pipette, leaving the neighboring wells (well 557 and 559) intact.

## Supporting Information

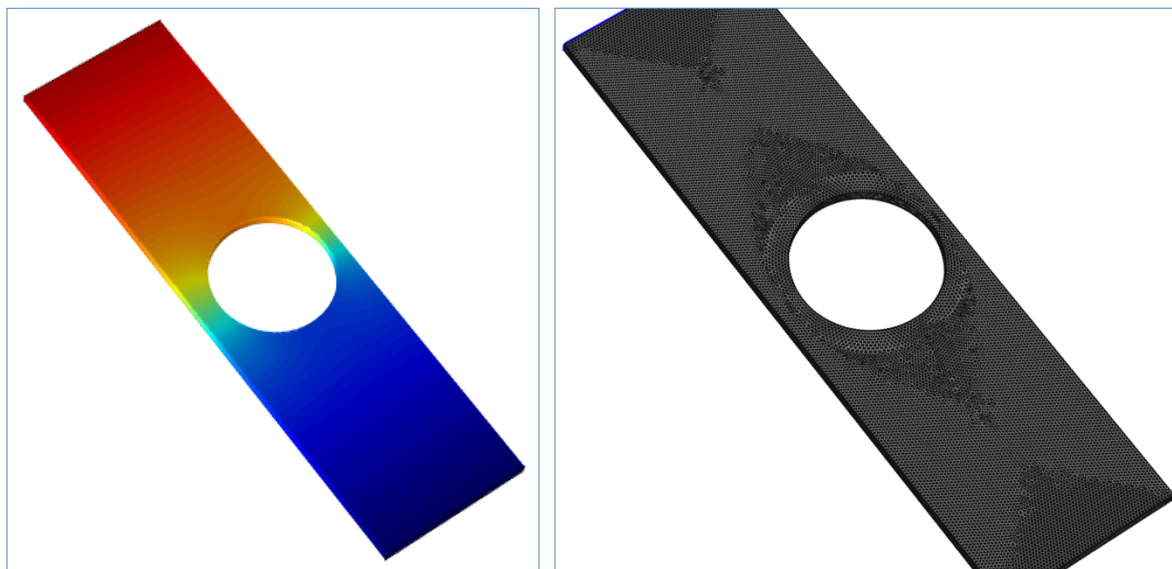


**Fig. S9** (Left) Color plot showing the pressure profile of the simulated flow (speed 0.001 m/s) through the channel; droplet occluding the channel is represented by the disc in the middle of the channel. Gradient goes from 158 Pa, in red, to 0 Pa, blue. (Right) Zoom in of the geometry simulated in the left panel, showing the finite-element mesh used.

BaVUL-F <sup>9</sup>	AAC CTG CCG TCT ACT CTT
BaVUL-R <sup>9</sup>	CAA CTG ACT TAA ACA TCC AT
8F <sup>10</sup>	AGAGTTTGATCCTGGCTCAG
1492R <sup>10</sup>	GGTTACCTTGTTACGACTT

**Table S1** Sequences of primers used in this paper

## Supporting Information

**Sanger sequencing from PWPCR product:**

>LMBV\_PWPCR

TGGCATCATGAGTCCGCATGTTACATGATTAAAGGTATTCCGGTAGACGATGGGGA  
TGC GTTCCATTAGATAGTAGGCGGGGTAACGGCCACCTAGTCTTCGATGGATAGGG  
GTTCTGAGAGGAAGGTCCCCACATTGGA ACTGAGACACGGTCCAAACTCCTACGG  
GAGGCAGCAGTGAGGAATATTGGTCAATGGGCGAGAGCCTGAACCAGCCAAGTAGC  
GTGAAGGATGACTGCCCTATGGGTTGTAACTTCTTTTATAAAGGAATAAAGTCGGG  
TATGCATACCCGTTTGCATGTACTTTATGAATAAGGATCGGCTAACTCCGTGCCAGC  
AGCCGCGGTAATACGGAGGATCCGAGCGTTATCCGGATTTATTGGGTTTAAAGGGA  
GCGTAGATGGATGT

## Supporting Information

**Partial 16s rDNA sequences of isolates:**

&gt;LM\_BV1

GTCGAGGGGCAGCATGGTCTTAGCTTGCTAAGACNGATGGCGACCGGCGCACGGGT  
GAGTAACACGTATCCAACCTGCCGTCTACTCTTGGACAGCCTTCTGAAAGGAAGATT  
AATACAAGATGGCATCATGAGTCCGCATGTTACATGATTAAGGTATTCCGGTAGA  
CGATGGGGATGCGTTCATTAGATAGTAGGGCGGGGTAACGGCCCACCTAGTCTTCGA  
TGGATAGGGGTTCTGAGAGGAAGGTCCCCACATTGGAAGTGGAGACACGGTCCAAA  
CTCCTACGGGAGGCAGCAGTGAGGAATATTGGTCAATGGGCGAGAGCCTGAACCAG  
CCAAGTAGCGTGAAGGATGACTGCCCTATGGGTTGTAACTTCTTTTATAAAGGAAT  
AAAGTCGGGTATGTATACCCGTTTGCATGTACTTTATGAATAAGGATCGGCTAACTC  
CGTGCCAGCAGCCGCGGTAATACGGAGGATCCGAGCGTTATCCGGATTTATTGGGTT  
TAAAGGGAGCGTAGATGGATGTTAAGTCAGTTGTGAAAGTTTGCGGCTCAACCGTA  
AAATTGCAGTTGATACTGGATATCTTGAGTGCAGTTGAGGCAGGCGGAATTCGTGGT  
GTAGCGGTGAAATGCTTAGATATCACGAAGAACTCCGATTGCGAAGGCAGCCTGCT  
AAGCTGCAACTGACATTGAG

&gt;LM\_BV2

ATGGCGACCGGCGCACGGGTGAGTAACACGTATCCAACCTGCCGTCTACTCTTGGAC  
AGCCTTCTGAAAGGAAGATTAATACAAGATGGCATCATGAGTCCGCATGTTACATG  
ATTAAAGGTATTCCGGTAGACGATGGGGATGCGTTCATTAGATAGTAGGGCGGGT  
AACGGCCCACCTAGTCTTCGATGGATAGGGGTTCTGAGAGGAAGGTCCCCACATTG  
GAACTGAGACACGGTCCAACTCCTACGGGAGGCAGCAGTGAGGAATATTGGTCAA  
TGGGCGAGAGCCTGAACCAGCCAAGTAGCGTGAAGGATGACTGCCCTATGGGTTGT  
AACTTCTTTTATAAAGGAATAAAGTCGGGTATGTATACCCGTTTGCATGTACTTTAT  
GAATAAGGATCGGCTAACTCCGTGCCAGCAGCCGCGGTAATACGGAGGATCCGAGC  
GTTATCCGGATTTATTGGGTTTAAAGGGAGCGTAGATGGATGTTAAGTCAGTTGTG  
AAAGTTTGCGGCTCAACCGTAAAATTGCAGTTGATACTGGATATCTTGAGTGCAGTT  
GAGGCAGGCGGAATTCGTGGTGTAGCGGTGAAATG

&gt;LM\_BV3

TGCAAGTCGAGGGGCAGCATGGTCTTAGCTTGCTAAGGCCGATGGCGACCGGCGCA  
CGGGTGAGTAACACGTATCCAACCTGCCGTCTACTCTTGGACAGCCTTCTGAAAGGA  
AGATTAATACAAGATGGCATCATGAGTCCGCATGTTACATGATTAAGGTATTCCG  
GTAGACGATGGGGATGCGTTCATTAGATAGTAGGGCGGGGTAACGGCCCACCTAGT  
CTTCGATGGATAGGGGTTCTGAGAGGAAGGTCCCCACATTGGAAGTGGAGACACGG  
TCCAACTCCTACGGGAGGCAGCAGTGAGGAATATTGGTCAATGGGCGAGAGCCTG  
AACCAGCCAAGTAGCGTGAAGGATGACTGCCCTATGGGTTGTAACTTCTTTTATAA

## Supporting Information

AGGAATAAAGTCGGGTATGCATACCCGTTTGCATGTACTTTATGAATAAAGGATCGGC  
TAACTCCGTGCCAGCAGCCGCGTAATACGGAGGATCCGAGCGTTATCCGGATTTAT  
TGGGTTTAAAGGGAGCGTAGATGGATGTTTAAAGTCAGTTGTGAAAGTTTGCGGCTCA  
ACCGTAAAATTGCAGTTGATACTGGATATCTTGAGTGCAGTTGAGGCAGGCAGGAAAT  
CGTGGTGTAGCGGTGAAATGCTTAGATATCACGAAGAAGTCCGATTGCGAAGGCAG  
CCTGCTAAGCTGCAACTGACATTGAGGCTCGAAAGTGTGGGTATCAAACAGGATTA  
GATACCCTG

## Supplementary References

1. T. M. Schmidt, [http://microbiomes.msu.edu/wp-content/uploads/2012/08/media\\_and\\_buffer\\_used\\_for\\_culturing\\_human\\_gut\\_microbiome.pdf](http://microbiomes.msu.edu/wp-content/uploads/2012/08/media_and_buffer_used_for_culturing_human_gut_microbiome.pdf), Accessed December 20, 2012.
2. F. Shen, W. Du, E. K. Davydova, M. A. Karymov, J. Pandey and R. F. Ismagilov, *Anal. Chem.*, 2010, **82**, 4606-4612.
3. W. Du, L. Li, K. P. Nichols and R. F. Ismagilov, *Lab Chip*, 2009, **9**, 2286-2292.
4. B. A. Kowert, N. C. Dang, J. P. Reed, K. T. Sobush and L. G. Seele, *Journal of Physical Chemistry A*, 2000, **104**, 8823-8828.
5. D. C. Duffy, J. C. McDonald, O. J. A. Schueller and G. M. Whitesides, *Anal. Chem.*, 1998, **70**, 4974-4984.
6. L. S. Roach, H. Song and R. F. Ismagilov, *Anal. Chem.*, 2004, **77**, 785-796.
7. R. R. Pompano, C. E. Platt, M. A. Karymov and R. F. Ismagilov, *Langmuir*, 2012, **28**, 1931-1941.
8. B. S. Stevenson, S. A. Eichorst, J. T. Wertz, T. M. Schmidt and J. A. Breznak, *Appl. Environ. Microbiol.*, 2004, **70**, 4748-4755.
9. Y. Miyamoto, K. Watanabe, R. Tanaka and K. Itoh, *Microbial Ecology in Health and Disease*, 2011, **14**, 133-136.
10. S. Turner, K. M. Pryer, V. P. W. Miao and J. D. Palmer, *Journal of Eukaryotic Microbiology*, 1999, **46**, 327-338.